

# Crack evolution in a frontal thermal protection: numerical analyses and experimental validation

*D. Schiariti\**, *F. Paglia\*\**, *E. Bellato\*\*\**, *G. Gonnella\*\*\*\**, *F. Di Cicco\*\*\*\*\**, *E. Lambiase\*\*\*\*\**,  
*G. Mastrangelo\*\*\*\*\**, *C. Dutertre\*\*\*\*\**, *E. Labarthe\*\*\*\*\**, *K. Mathis\*\*\*\*\**

*\*AVIO SpA, via Ariana km 5.2-Colleferro (Rome), Italy 0034*

*daniele.schiariti@avio.com*

*\*\* AVIO SpA, via Ariana km 5.2-Colleferro (Rome), Italy 0034*

*fabio.paglia@avio.com*

*\*\*\* AVIO SpA, via Ariana km 5.2-Colleferro (Rome), Italy 0034*

*enrico.bellato@avio.com*

*\*\*\*\* AVIO SpA, via Ariana km 5.2-Colleferro (Rome), Italy 0034*

*giampiero.gonnella@avio.com*

*\*\*\*\*\* AVIO SpA, via Ariana km 5.2-Colleferro (Rome), Italy 0034*

*fabrizio.dicicco@grade.avio.com*

*\*\*\*\*\* AVIO SpA, via Ariana km 5.2-Colleferro (Rome), Italy 0034*

*emanuele.lambiase@avio.com*

*\*\*\*\*\*Europropulsion, 11, rue Salomon de Rothschild, Suresnes,(France)*

*giorgio.mastrangelo@europropulsion.com*

*\*\*\*\*\* ESA HQ Daumesnil, 48-56 rue Jacques Hillairet, Paris,(France)*

*charline.dutertre@esa.int*

*\*\*\*\*\* CNES, 2, Place Maurice Quentin, Paris,(France)*

*emilie.labarthe@cnes.fr*

*\*\*\*\*\* CNES, 2, Place Maurice Quentin, Paris,(France)*

*kevin.mathis@cnes.fr*

## Abstract

In this paper, a numerical study and experimental validation concerning the crack propagation in a frontal thermal protection (PTF) during combustion in solid rocket motors is presented. After a full-scale bench firing test, PTF showed unexpected cuts and over-erosions at the expertise. Avio S.p.A. has developed a methodology to explain the crack propagation and to evaluate the relevant Structural and Thermal Safety Factors. A 3D fluid-structure interaction analysis has been performed to study the fluid-dynamic behaviour of the PTF. Fracture mechanics approach and progressive failure methodology have been combined to reproduce by FEM the crack propagation on PTF elastomeric material.

## 1. Introduction

The ARTA05 PTF S3 configuration was chosen in the frame of activities aimed to achieve the technical solution for a reduction and stabilization of the ODP levels of MPS. Main aim was to definitely solve the anomaly observed, for the first time, on the flight L541. Due to this anomaly the flight levels exceeded the ODF levels specified in MPS DF, which are at the basis of the launcher qualification, for the 3<sup>rd</sup> blast of the 1<sup>st</sup> and 2<sup>nd</sup> acoustic modes. A technical solution aimed to decrease the maximum expected level of OdP 3<sup>rd</sup> peak to levels compatible with the system qualified reference has been identified: reduction of the floater and frontal PTF thickness. This solution was successfully applied on the ARTA05 firing test obtaining a substantial margin with respect to the ODP launcher qualification limits. Nevertheless, ARTA05 PTF S3 showed, on two regions, tearing and extra erosions not predicted by the 2D axial-symmetric models used to justify the new ARTA05 PTF. Tearing and the extra erosions have to be understood and explained, with the aim to justify that their occurrence is not critical for the MPS. Two different geometrical configuration have been identified for the FSI and structural analyses:

- Configuration # 1 : PTF at closed floater;
- Configuration #2 : PTF at opened floater.

Aim of the present paper is to summarize all the performed activities relevant only to the case closed floater (configuration #1) and to demonstrate that the occurrence of tears on the PTF doesn't affect the Propellant Thermal and Structural Safety Factor. The following activities have been performed in order to complete the technical justification:

- Thermal and Fluid Dynamics Justification;
- Testing;
- Structural Justification.

Thermal and Fluid Dynamics Justification consisted in a full 3D fluid-structure interaction analysis (FSI), performed in order to study the fluid-dynamic behaviour of the PTF with the presence of a crack, by using an in-house developed code. The Structural Justification and Testing consisted in the application of fracture mechanics approach and progressive failure methodology combined together to reproduce the crack propagation on an elastomeric material. Laboratory tests and small scale tests have been performed to identify the material constitutive law and to reproduce the modes #1 and #3 break on tearing test by FEM. The two modes of break (see Figure 1) have been investigated because the expected crack propagation on PTF is due to a combination of these tearing modes. The logic followed during the justification activities is summarized in a flow-chart reported in Figure 2. The following success criteria have been taken into account:

- **Tearing Tests and Small Scale Tests:** A difference lower than 30% for each mode of break is acceptable to consider the FEM model correlated and able to capture and reproduce the crack evolution. This value is due both to the dispersion obtained by experimental tests (20% on displacement and 10% on load, see chapter 3) and to the Avio experience on composite material (20%); it is challenging taking into account that the 20% for composite material is for a static response. The difference of 30% is the maximum allowable value linked to the test parameters and so it is not affected by the fact that the Mode #1 and #3 are correlated separately on the small scale tests;
- **FSI/Structural Cross-Check:** The difference between the delta pressure obtained by FSI and the minimum delta pressure given by FEM analysis able to cause crack propagation have to be lower 30%.

## 2. FSI-thermal justification analysis

The PTF inside the booster is a highly deformable structure that requires the study of the interactions between the fluid dynamics and the structural mechanics. The FSI main feature is the movement of the fluid boundary under the action of the fluid itself. A full coupling is required between the fluid dynamics and the structural mechanics. This coupling happens through a fluid-structure interface, where a bilateral force exchange between the fluid and the structure takes place. The purpose is to obtain the deformed configuration, the heat fluxes and the pressure distributions along the PTF in the no-tear and tear case in order to evaluate the thermal Safety Factor (thermal SF) and the delta pressure between front and rear side of PTF. The no-tear case is the nominal one while in the tear case there is one long and thin cut in order to simulate a crack propagation up to the propellant grain (the worst case). A specific time instant to be used for the FSI and structural analyses with closed floater has been identified. It has been chosen the configuration in which the protrusion between the tip and the propellant grain is maximum; the delta pressure acting on the surface is relevant. The PTF has been modelled taking into account the eroded geometry corresponding to the identified time instant. Therefore two FSI analyses have been performed (no-tear case and tear case) at a specific burning instant.

### 2.1. FSI numerical methodology

The adopted coupling methodology is the partition treatment. Selected because it enables the use of different commercial codes for the CFD and structural analyses and it allows an easy use of a non-matching discretization. This methodology consists in solving the fluid dynamic and the structural domains with two separated models, coupled through an explicit data exchange module (each module transfers the data only when the convergence is reached). The FSI iterative procedure can be synthesized in the following 5 steps:

1. The CFD solver calculates the fluid-dynamic field;

2. The pressure is transferred on the structural domain;
3. The structural solver calculates the structural deformation field;
4. The deformations are transferred on the fluid-dynamic domain;
5. The loop restarts from the step 1 until the convergence is reached.

At each iteration, since the structure deformation modifies the CFD boundary, the domain has to be re-meshed before the fluid dynamic analysis. The CFD grid and structural grid are not matched that is the structural nodes are not coincident with the fluid-dynamic ones, thus requiring some interpolation procedures for data exchange. The data interpolation of the properties (that is the pressure and displacement values) is performed by means some Matlab functions (in-house developed codes). A triangular grid is generated starting from the structured mesh. After that there is an association between every host triangular element and the closest guest node of the destination mesh (example in Figure 3). Finally, the property is transferred from the host element to the guest node by means shape functions of the triangular element. The guest node is projected onto the triangular host element and takes the property value in that point of the field (Figure 4). Fluid dynamic simulations have been accomplished by means of the numerical commercial CFD tool Ansys. All the numerical simulations have been conducted according to the following hypotheses: steady state approach, second order integration accuracy, K- $\epsilon$  turbulent flow model with standard wall function, advancing implicit scheme, density based solver, compressible flow. The condition for the CFD analysis corresponds to the un-deformed configuration. Regarding the heat fluxes evaluation a refinement of the mesh has been performed after the FSI analysis in order to reach the appropriate value of wall  $y^+$ . Structural analyses have been performed by means of the solver FEM code MARC. For all the developed analyses, the following hypotheses have been assumed: large strain approach, full Newton-Raphson iteration, the mesh used is structured.

## 2.2. FSI results

The computational domain (Figure 5) includes the S2 and S3 segment of the booster, the mass flow inlet is imposed on the propellant grain surfaces and pressure is set in outlet. In Figure 6 are shown the deformations of PTF (tear case) during the loop iterations; it can be noticed that the values of deformation near the cut are greater with respect to the deformations far from the cut. There has been high variability of the displacements near the cut during the FSI iterations because the local pressure gradient (due to the cut) makes this area more sensitive. In Figure 7 are reported the results for the front side of the PTF. For the no-tear case, the behaviours are regular and axisymmetric: the heat fluxes increase toward the tip while the pressures have the opposite trend. For the tear case, near the cut the heat fluxes increase toward the tip more quickly with respect to the no-tear case. Similarly also the pressure values decrease toward the tip more quickly with respect to the no-tear case because of the greater deformation in the cut area. It can say that the presence of the tear yields a local effect in the cut area only. The maximum delta pressure between the front and rear side in the tear case has been evaluated and used for FSI-structural crosscheck. This value is referred to both the effects of mode 1 and 3, therefore it is not possible to distinguish the two contributes; nevertheless the mode 1 effect is predominant. The heat fluxes evaluated in the no-tear and tear case by means CFD analyses have been utilized to obtain the thermal safety factor (SF) on PTF surface. The thermal SF has been evaluated in the region around the tear because of the higher heat fluxes with respect to the no-tear case. This represents the worst case because in this configuration the tear reaches the propellant grain. For the evaluation only the control points close to the propellant grain are taken in account (point 1-2). The other control points are not considered because there is no more propellant grain in correspondence of these points. Thermal SF are higher than 1,3 as prescribed by thermal requirements in the current production phase. A reduction of about 12.6% has been estimated with respect to the no-tear case.

It is worth noting that the real values have to be considered higher than the obtained ones. In fact, as it is showed in the structural/FSI crosscheck the length of the maximum propagated crack is shorter than the tear length hypothesized for the FSI analysis. Therefore the local effect does not reach the area in correspondence of the propellant grain. Consequently the thermal safety factor in the two control points can be considered nearly the nominal one (no-tear case).

## 3. Experimental tests

Several analyses have been performed in order to identify the PTF elastomeric material constitutive law on the basis of Laboratory Tensile and Tearing tests. The results obtained by tensile tests, performed for different rubber thicknesses, have been adopted to reproduce by FEM the tearing test experimental data. In particular, the numerical models of lab test specimens for both modes (#1 and #3) break have been performed with the following inputs:

- the constitutive law obtained by Tensile Tests results;
- the identified progressive failure criteria based on maximum Von Mises Stress.

Hereafter, the performed experimental tests have been described in detail.

### 3.1 Tensile tests

Stress-Strain curves for the PTF elastomeric material have been obtained by tensile tests performed on Afnor specimens at ambient Temperature and with crosshead speed of 500 mm/min according to [1]. The tensile tests have been executed with three different thicknesses (2, 4 and 5 mm), in order to verify the variability of the mechanical characteristics with the thickness; the test matrix is reported in Table 1. The results obtained by tensile tests allowed to identify the constitutive law for the PTF elastomeric material to be used as input in the FEM. The normalized Stress-Strain curves have been reported in Figure 9 as example.

### 3.2 Tearing tests

Tearing tests have been performed for both Mode #1 and #3 break following [2]. The test specimen utilized for the Mode #1 has a Type C geometry (see Figure 10), an un-nicked test piece with a 90° angle on one side and with tab ends. The force acts on the test piece in a direction substantially parallel to the tab ends of the specimen (45° to the 90° center angle) in the direction of grip separation. The test specimen utilized for the Mode #3, instead, has a Type T geometry (as shown in Figure 10); for this specimen, tear propagation is measured in the direction parallel to the length of both legs. Several specimens have been manufactured and tested for different thickness values (2, 4 and 5 mm, as reported in Table 2); all the tests have been performed at ambient Temperature and with the corresponding crosshead speed specified in [2] (see Figure 11). The tearing tests results have been used to validate by FEM the identified constitutive law (see chapter 4).

### 3.3 Small Scale Tests

The expected crack propagation on PTF is due to a combination of both tearing modes (Mode #1 and #3); therefore two small scale tests have been necessary to study the two modes separately, in this way, it is been possible to take into account (and evaluate) each percentage contribution of Mode #1 and #3 of solicitation to the stress field, which it would be impossible with a correlation based on a single small scale test with combined mode of solicitation (#1 + #3). Two dedicated Small Scale Tests have been performed in order to study the crack propagation under Mode #1 and #3 solicitation and to build a proper database for the validation of the structural model. On the basis of the constitutive law identified in the preliminary phases and validated by FEM (see § 4.1), two small scale test configurations have been identified via FEM analyses (see § 4.2): a Circular Sheet with constant thickness (Mode #1) and a small scale PTF (Mode #3); both the test items have been made with the same elastomeric material used for the ARTA05 PTF manufacturing and have been provided of initial crack triggers (1 single crack on the Circular Sheet and 2 identical cracks on the small scale PTF). The Mode #1 Small Scale Test has been performed on a Rubber Circular Sheet with a constant thickness instead on a small scale PTF. In fact, preliminary FEM analyses demonstrated that the crack propagation for only Mode #1 tearing on PTF small scale would be not feasible. So, it's been necessary to conceive a different test item for the Mode #1 Small Scale Test. The new small scale test configuration (Rubber Circular Sheet with constant thickness) is suitable to demonstrate the FEM correlation for Mode #1 tearing, it is easy to implement and will allow to predict the crack propagation for Mode #1 tearing on PTF full scale. In particular, the test have been executed as follows:

- **Mode #1 break:** A tapered wedge, made in Aluminum alloy, pushed into the inner hole of a Circular Sheet with constant thickness to cause crack propagation (see Figure 12);
- **Mode #3 break:** An eccentric tapered wedge (also made in Aluminum alloy) have been installed on the same wedge used for Mode #1 to cause the propagation of the initial cracks of the small scale PTF under Mode #3 of loading (see Figure 12).

The boundary conditions and dimension of crack triggers for each small scale test are compliant with the structural analyses performed to predict the test results and reported in the § 4.2. The Circular Sheet, for Mode #1 test, has been mapped with concentric circles to verify instantly the crack evolution. A number of 6 potentiometers have been arranged on circular sheet in order to record the displacements and the cracks opening during the test (see Figure 14).

The position of the potentiometers has been chosen on the basis of the crack path predicted by FEM. The Small Scale PTF has been instrumented by means of 2 potentiometers. The potentiometers bodies have been installed on the test machine, while the two respective pins have been attached on the PTF (see Figure 15). Both small scale tests have been performed at ambient Temperature. The testing machine, purposely made for the small scale tests, is shown in Figure 13. The machine has a tapered wedge able to move in axial direction with a crosshead speed of 500 mm/min and a clamping system for Circular Sheet and Small Scale PTF in agreement to the FEM simulations performed to predict the test results (see § 4.2). A removable eccentric tapered wedge and a dedicated clamping system allow to simply switch between Mode #1 and Mode #3 test configurations. An electronic display shows the wedge position and the reaction force. Small Scale PTF and Circular Sheet have been examined with U.S. control system before the test, in order to assure the absence of pre-existent defects inside the items in test.

## 4. Structural analyses

The identified constitutive law for PTF elastomer has been applied on 3D numerical models to reproduce the laboratory Tearing Tests and Small Scale Tests results. The correlation between numerical and experimental data allowed to validate the identified constitutive law. Once validated for both laboratory and small scale tests, the same identified constitutive law has been applied on 3D FEMs of the ARTA05 PTF in configuration at closed floater in order to identify the delta pressure able to cause the crack growth on the PTF and the minimum angular position (on the PTF) at which is possible to generate another tear. Hereafter, the numerical models and the corresponding results have been reported for each analysed case.

### 4.1. FEM and correlation for tearing tests

3D FEMs of the Mode #1 and #3 Tearing Tests specimens have been performed for each thickness value, adopting hexahedral 8 nodes elements with full integration. The material properties have been implemented with a Mooney material formulation; the Mooney coefficients have been determined using the stress-strain curves obtained by tensile tests. The boundary conditions have been applied to Master Nodes connected to the Slave ones corresponding to the grip zone on the specimens. A full clamping is applied to the region corresponding to the fixed side of the specimen, while the moving side is also fully clamped except for the load applying direction. The load, in terms of imposed displacement, is applied to the corresponding Master Node and transferred to the Slave ones. All the performed structural analyses are Non-Linear. The failure criteria for rubber crack propagation is based on maximum allowable Von Mises Stress; a dedicated Fortran subroutine apply for each time-step of the simulation the failure criteria. The maximum allowable Von Mises Stress considered for the crack propagation has been identified as optimal for experimental data fitting w.r.t. the applied load (force). The structural analyses results performed on the Mode #1 and #3 Tearing Tests (Numerical Load vs Displacement curves), compared with the corresponding experimental data, have been displayed in Figure 18 as example (normalized values). The contour plot with the crack evolution is reported in Figure 17 for both tearing modes. It is possible to notice the good correlation between FEM and experimental results. In fact, the maximum obtained difference (expressed as absolute values w.r.t. the applied load) is 9% for the Mode #1 and 10% for the Mode #3. The maximum differences for each examined case are displayed in Table 3. The success criteria for FEM validation is a difference lower than 30% between experimental and numerical data, which is widely satisfied by the obtained results. In fact, the Applied load vs Displacement curves, all obtained with the same constitutive law, present a difference with the experimental data always lower than 10%; the identified constitutive law is able to fit the PTF elastomeric material behaviour independently by the thickness used. Therefore, the identified constitutive law (property of PTF elastomeric material) has been validated at Lab Test level and can be applied for the simulation on Small Scale and Full Scale ARTA05 PTF.

### 4.2. FEM and correlation for small scale tests

3D numerical models have been performed for each configuration in order to predict the small scale tests results. Non-linear analyses have been performed with 3D FEMs using hexahedral 8 nodes elements with full integration and contact bodies; the constitutive law is the same used for the Tearing Tests numerical modelling. In both cases (Small Scale Test configuration for Mode #1 and #3 break), a Master Node is connected to Slave Nodes on the tapered wedge (red regions in Figure 19 and Figure 23); the load, in terms of imposed displacement, is applied to the Master Node that transfers the load to the wedge causing its moving and penetration through the inner hole of the test item.

#### 4.2.1 FEM for Mode#1 small scale test

The FEM for Mode #1 propagation consists of a Circular Sheet and a Tapered Wedge. The Circular Sheet, item in test, has a 5 mm thickness and is clamped on the external radius (pink region in Figure 19). The presence of an initial crack localized on the internal radius has been also simulated in the model. The choice of the initial crack length is made on the basis of preliminary analyses that showed this configuration as optimal for crack propagation compatibly with the reaction force involved during the test. The material properties have been implemented with a Mooney material formulation; the Mooney coefficients have been determined using the stress-strain curves obtained by tensile tests and validated at Lab Test level. The FEM structural analyses results evidenced the propagation of the initial crack and the birth of a second crack that propagated in a direction opposite to the first one. The FEM results with contour plot and crack evolution for Mode #1 break are reported in Figure 20.

The Circular Sheet, after the Mode #1 test, presented a final crack length and shape compliant with the one predicted by FEM simulation as shown in Figure 21; as expected before the test, the cracks passed between the potentiometers bodies and the respective pins, allowing to record the crack opening. The maximum difference between experimental and numerical final cracks length, expressed as absolute value, is 14.06%. Moreover, to confirm the FEM capability to predict the crack evolution (step by step), further correlations between experimental and numerical data have been performed:

- Crack Length vs Wedge Displacement curves (normalized values), displayed in Figure 22;
- Reaction Force vs Wedge Displacement curves (normalized values), showed in Figure 27.

The maximum difference between numerical and experimental data is showed in Table 4 in terms of absolute values for each analyzed magnitude; the maximum detected difference is 25%, lower than the acceptable value of 30%. So, the identified constitutive law for the PTF elastomeric material allow to reproduce by FEM the Mode #1 Small Scale Test.

#### 4.2.2 FEM for Mode#3 small scale test

The FEM for Mode #3 propagation consists of an Eccentric Tapered Wedge and a Small Scale PTF (test item). The PTF has been clamped (green region in Figure 23) in order to leave a free deformable circular region compliant (in the chosen scale) with the ARTA05 PTF in configuration with closed floater. Two cracks have been simulated in the model as trigger for propagation; an additional clamping in correspondence of these initial cracks has been applied into the model (yellow region in Figure 23). The choice of the initial cracks length and angular distance, similarly as did for the Mode #1, is made on the basis of preliminary analyses that showed this configuration as optimal for crack propagation compatibly with the reaction force involved during the test. The material properties have been implemented with a Mooney material formulation; the Mooney coefficients have been determined using the stress-strain curves obtained by tensile tests and validated at Lab Test level. The FEM structural analyses results evidenced the crack propagation in radial direction for both initial tears. The FEM results with contour plot and crack evolution for Mode #3 break are reported in Figure 24. The Small Scale PTF, after the Mode #3 test, presented a final crack length and shape compliant with the one predicted by FEM simulation as shown in Figure 25. The maximum difference between experimental and numerical final cracks length, expressed as absolute value, is 4.83%. Analogously to the Mode #1, further correlations between experimental and numerical data have been performed to confirm the FEM capability to predict the crack evolution (step by step):

- Crack Length vs Wedge Displacement curves (normalized values), showed in Figure 26;
- Reaction Force vs Wedge Displacement curves (normalized values), displayed in Figure 27;

The maximum difference between numerical and experimental data is showed in Table 4 in terms of absolute values: the maximum detected difference is 20.27%, lower than the acceptable value of 30%. So, the identified constitutive law for the PTF elastomeric material allow to reproduce by FEM also the Mode #3 Small Scale Test. Therefore, the identified constitutive law (property of PTF elastomeric material) has been validated at Small Scale level and can be applied for the simulation on 3D numerical models of the Full Scale ARTA05 PTF.

### 4.3 FEM for ARTA05 PTF

The same methodology validated at Lab Test level (Mode #1 and #3 Tearing Tests) and Small Scale Test level (Mode #1 and #3 break) has been applied for the numerical modelling of the ARTA05 PTF, in order to:

- identify the delta pressure able to cause the crack growth on the PTF;

- identify the minimum angular position (on the PTF) at which is possible to generate another tear.

On the basis of the experimental results of ARTA05 and taking into account the experience of the fluid-dynamic behaviour rebuilt for ARTA03 and ARTA04 PTF3D a closed floater dimensioning configuration has been identified. The dimensioning configuration corresponds to the max PTF protrusion w.r.t. propellant grain; this time instant is dimensioning in terms of stress level and crack propagation over the propellant due to the high exposed PTF surface and the relevant delta pressure acting on it. The dimensioning configuration has been analysed for different length of crack, in order to identify its critical value and the stability condition. The expected crack propagation on PTF is due to a combination of both tearing modes (Mode #1 and #3, even if, as afterwards explained, the Mode #1 is the predominant). In the Mechanics of Fracture approach and Crack Growth analyses, when a multi-axial loading occurs, the contribution of each mode of loading is usually evaluated separately and then combined. Similarly, in the proposed methodology, the contribution of each mode has been calculated separately (in terms of stress), and then combined together, taking into account of the dimensioning load conditions and evaluating the influence of each mode of loading. The contribution of each mode, in fact, has been weight in function of pressure field on PTF using the dedicated Fortran subroutine (validated on lab and small scale tests) that for each time-step compared the allowable with induced stress and identified the crack propagation.

Non-Linear analyses have been performed with 3D FEMs of the ARTA05 PTF using hexahedral 8 nodes elements with full integration. The PTF has been modelled taking into account the eroded geometry corresponding to the identified time instant. A full clamping has been applied as shown in Figure 28, in order to leave a distance between propellant grain and tip compliant with the PTF in the chosen configuration. Two different pressure fields (see Figure 29) have been applied in order to identify the delta pressure able to cause the crack growth on the PTF:

- The first has been applied on the front surface of the PTF in order to cause a Mode #1 loading;
- The second has been applied on half of the PTF front surface in order to cause Mode #3 loading;

The same constitutive law validated on Lab Tests and Small Scale Tests has been implemented in the model with a Mooney material formulation (which coefficients have been derived from the Stress-Strain curves obtained by tensile tests) to simulate the PTF elastomer behaviour. The allowable stress, for the dimensioning load conditions, has been calculated taking into account the temperature effect on the crack tip. A mechanical characterization has been performed up to a conservative temperature to avoid the degradation phenomena of PTF rubber due to its EPDM elastomeric nature. All the analyses have been performed under the assumption that the rubber in correspondence of the crack tip remained intact and not degraded. The performed progressive failure analyses have been executed considering only the propagation due to mechanical causes and ignoring the erosion phenomena. In fact, when the erosion phenomena occurs, the shape of crack tip changes and it is not possible to apply the fracture mechanics standard approach. Several analyses have been performed for different tear length; the obtained FEM results allowed to identify a range of length and corresponding delta pressures compatible with the crack growth on the ARTA05 PTF in configuration at closed floater. The equivalent delta pressures have been evaluated and confirmed by FEM analyses for each crack length taking into account the contribution of each mode of loading. These values will be compared with the maximum delta pressure given by FSI analyses for the cross check correlation (see chapter 5). The contour plot with crack propagation for the ARTA05 PTF is showed as example in Figure 30. The Crack Length vs Propagation Delta Pressure curves have been reported for Mode #1, Mode #3 and Mode #1+#3 in Figure 31(normalized values). The results obtained by FEM have evidenced that:

- A spontaneous crack in this configuration can't be generated with the considered pressure field;
- Exist a range of crack length and corresponding delta pressures compatible with crack growth on the ARTA05 PTF in configuration at closed floater;
- Exist a critical value for the crack length; starting from this value, the delta pressure able to cause crack propagation is constant and it is the minimum identified value;
- Exist a crack length which correspond to the stability point for the crack growth; starting from this value, the delta pressure able to cause crack propagation increase quickly;
- The maximum crack length obtained with the considered load conditions is 18 mm lower respect to the propellant position. Therefore, the crack can't reach the propellant grain in this configuration (closed floater);
- No additional tear is compatible with the analyzed pressure field; the Von Mises stress distribution is uniform far from the crack and the angular position which is potential for the generation of a second crack is between 45-180 degrees (zone with maximum Von Mises Stress field). A second tear (and consequent crack growth) could be explained by the presence of a defect induced by the combustion process on the PTF or analyzing the opened floater configuration;
- The Mode #1 loading is predominant w.r.t. the Mode #3, as demonstrated by FSI analyses (see chapter 2).

## 5. FSI/Structural cross-check

The results of the Structural and FSI analyses have been compared in order to verify if the final delta pressure between front-rear side can explain crack propagation. The analyses performed during Structural Justification evidenced that exists a pressure field able to cause the crack propagation; a spontaneous crack generation isn't compatible with the load conditions considered for the analyzed configuration. The analyses performed during the FSI allowed to determine a maximum delta pressure acting on the PTF inside the segment. This value is compliant with the equivalent delta pressure able to generate crack propagation in the range of instability of the crack. In this range, the delta pressure evaluated by FEM has a maximum difference of 28% with respect to the FSI value, lower than the 30% defined as success criteria; out of this range, the delta pressure isn't able to cause the crack growth. In Figure 32, the nominal delta pressure obtained by FSI analysis augmented of 30% (blue band) fits the equivalent delta pressure compliant with the crack propagation obtained by structural analysis in the instability crack length range. The maximum possible crack length with the considered load conditions is 126 mm lower respect to the propellant position; therefore, the crack tip is not able to reach the propellant grain under the delta pressure acting inside the segment. The structural Safety Factor for the PTF with closed floater configuration in correspondence of propellant grain is greater than 2. The values of the thermal safety factors are higher than 1.3. As previously said, these values have been evaluated considering the tear up to the propellant grain; as evidenced by the structural analyses, the crack can't reach the propellant grain and consequently the thermal fluxes in that zone are lower. The evaluated thermal safety factors are conservative, the values can be considered nearly the nominal ones. So, there are no impacts on the Propellant Thermal and Structural Safety Factors. A second crack can't be generated with the delta pressure obtained from the correlation between FSI and structural analyses, being the Safety Factor for the birth of another tear always greater than 3. The Von Mises stress distribution is uniform far from the crack; the minimum angular position for the crack generation could be between 45÷180 degrees for the configuration at closed floater. As second tear (and consequent crack growth) could be explained by the presence of a defect induced by the combustion process on the PTF or analysing the opened floater configuration.

## 6. Conclusions

The FSI and CFD analyses of the PTF without tear and with the presence of the tear have been performed; they evidenced that with the presence of the tear there is a local variation of the heat fluxes and pressures only in the cut area. The maximum delta pressure between front and rear side along the cut was identified and compared to the structural value; the heat fluxes increase along the cut because of the more elevated convective exchange; the thermal safety factors of the control points close to the grain propellant have been evaluated and are higher than 1,3 as prescribed by the thermal requirements during the current production phase. But considering the structural results, the maximum crack propagation does not reach the propellant grain, therefore the heat fluxes on the PTF in the zone of interest are lower. Consequently the thermal SF in the two control points can be considered nearly the nominal one.

The constitutive law identified by Tensile Tests allowed to correctly reproduce the PTF elastomer behaviour and crack propagation. In fact, the maximum difference obtained between Experimental and Numerical Load vs Displacement curves are, respectively for Mode #1 and Mode #3, 9% and 10% (in terms of absolute values); these values are lower than the allowable difference of 30% defined as success criteria. Two different configurations for the Mode #1 and #3 Small Scale Tests have been identified by FEM analyses. The 3D FEM analyses, performed using the same constitutive law validated with lab tests, allowed to predict the Small Scale Tests results and to define the Testing Machine specifications. The experimental tests results have been compared with the numerical prediction in terms of Displacements, Reaction Force, Crack Propagation and Final Cracks Length. The maximum difference between experimental and FEM results are, respectively for Mode #1 and #3, 25% and 20.27% (in terms of absolute values); these values are lower than the allowable difference of 30% defined as success criteria. Therefore, the identified constitutive law (property of PTF elastomeric material) has been validated. The same methodology validated on Lab Tests and Small Scale Test has been applied for the analyses performed on the 3D FEMs of ARTA05 PTF in closed floater configuration.

A cross check between FSI and structural analyses has been performed. The nominal delta pressure obtained by FSI analysis augmented of 30% (defined as success criteria) fits the equivalent delta pressure compliant with the crack propagation obtained by structural analysis in the instability crack length range. So, inside this range, crack propagation is it possible with the delta pressure acting on the PTF inside the segment. The maximum possible crack length with the considered load conditions is 126 mm lower respect to the propellant position. Therefore, the crack can't reach the propellant grain in this configuration (Closed Floater).

The structural Safety Factor for the PTF with closed floater configuration in correspondence of propellant grain is greater than 2; the thermal Safety Factor, instead, in correspondence of propellant grain is greater than 1.3 and nearly the nominal value. So, there are no impacts on the Propellant Thermal and Structural Safety Factors. A second crack can't be generated with the delta pressure obtained from the correlation between FSI and structural analyses, being the Safety Factor for the birth of another tear always greater than 3. The Von Mises stress distribution is uniform far from the crack; the minimum angular position (zone with maximum Von Mises Stress) for the crack generation could be between 45÷180 degrees for the configuration with closed floater. A second tear (and consequent crack growth) could be explained by the presence of a defect induced by the combustion process on the PTF or analysing the opened floater configuration.

## 2. Figures and tables

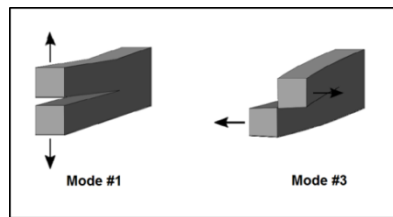


Figure 1: The modes (Mode#1 and Mode#3)

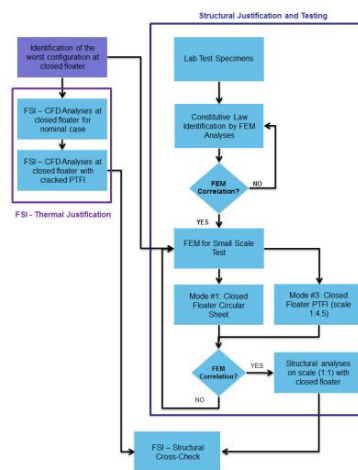


Figure 2: Justification logic flow chart

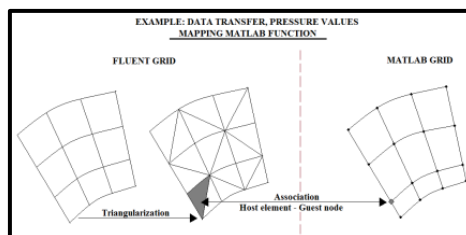


Figure 3: Example of host-guest association

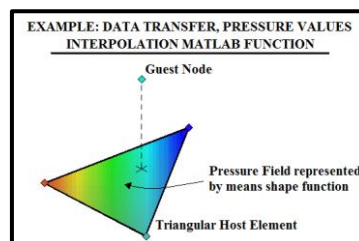


Figure 4: Property Interpolation

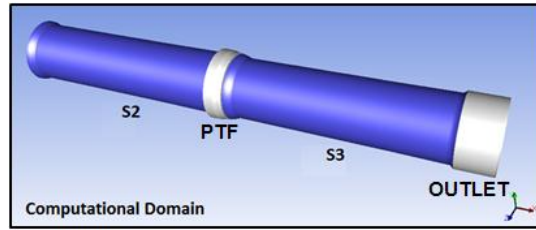


Figure 5: Computational domain

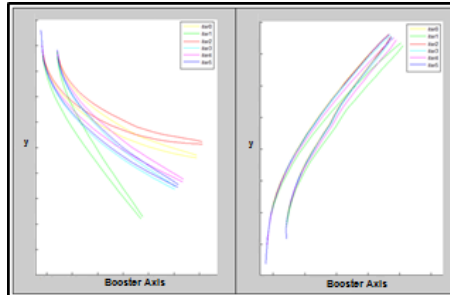


Figure 6: Deformations near the cut (left); far from the cut (right)

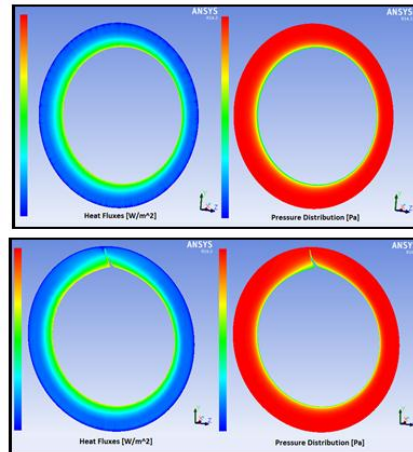


Figure 7: Heat fluxes and pressure distributions in the front side of PTF; no-tear case (up); tear case (down)

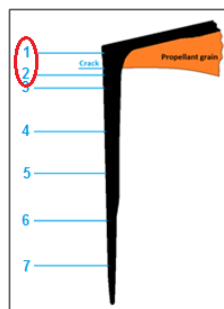


Figure 8 Control points

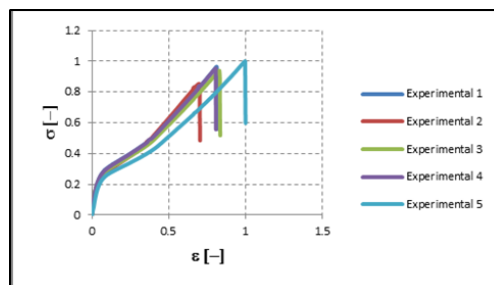


Figure 9: Stress-strain curves obtained by tensile test

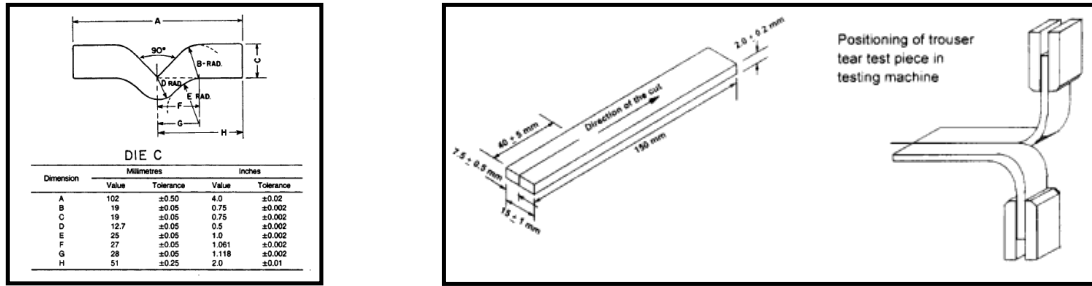


Figure 10: Mode #1 (on the left) and #3 (on the right) Tearing Tests Specimens



Figure 11: Mode #1 (on the left) and #3 (on the right) Tearing Tests

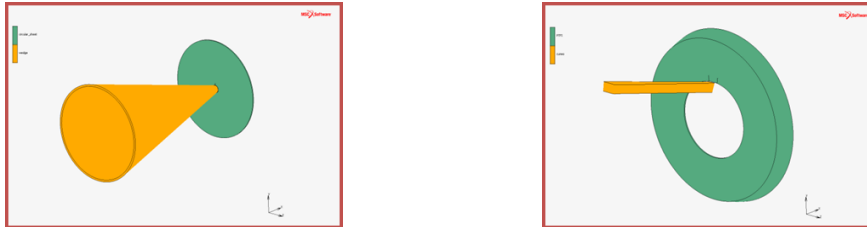


Figure 12: Mode #1 (on the left) and #3 (on the right) Small Scale Test Configurations



Figure 13: Testing machine used for both Mode #1 and #3 small scale tests. In the low, the small scale PTF

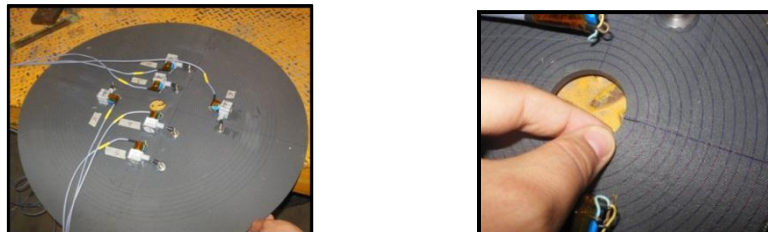


Figure 14: Potentiometers position on the circular sheet and detail of the initial crack



Figure 15: Potentiometers pins position and detail of the initial cracks on the small scale PTF

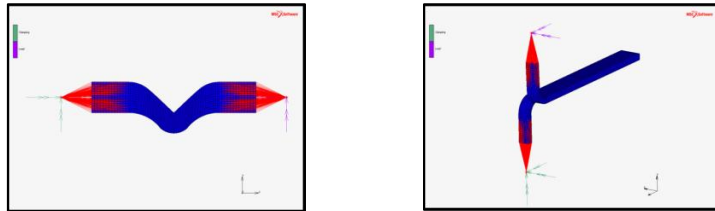


Figure 16: FEM for Mode#1 (on the left) and #3 (on the right) Tearing Test Specimens

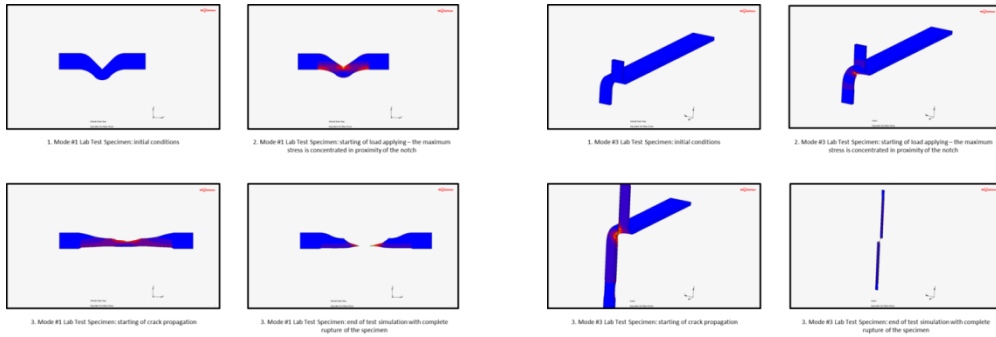


Figure 17: Crack evolution for Mode#1 (on the left) and #3 (on the right) Tearing Tests 3D numerical models

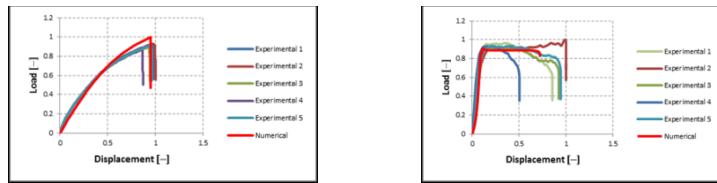


Figure 18: Load vs displacement curves for Mode#1 (on the left) and #3 (on the right) Tearing Tests

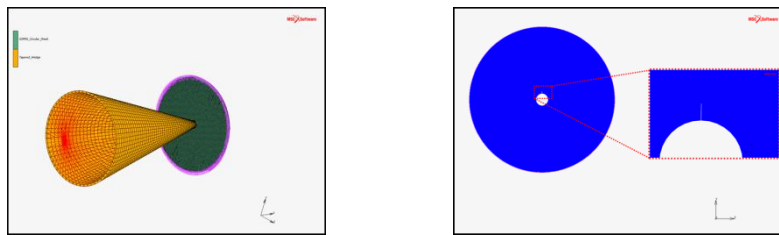


Figure 19: 3D FEM representative of Mode#1 Small Scale Test

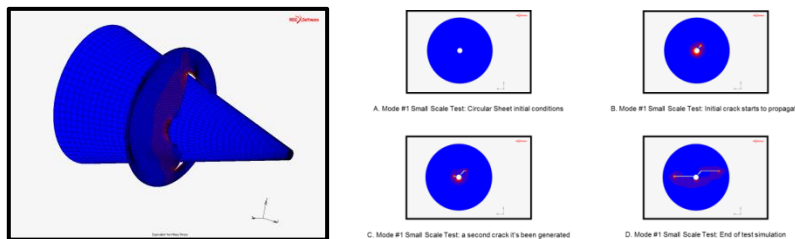


Figure 20: FEM results for Mode#1 Small Scale Test

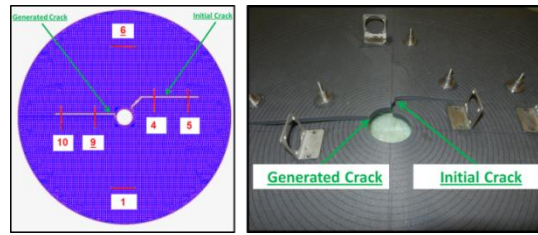


Figure 21: Crack shape, final crack length and potentiometers position for Mode#1 break: Numerical vs Experimental results

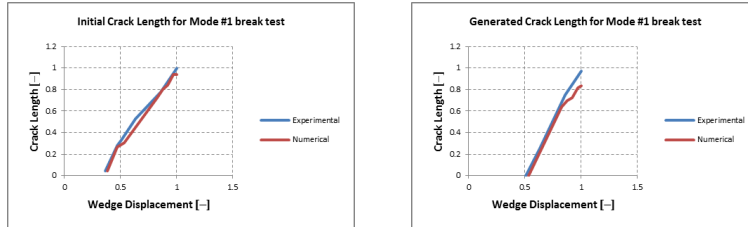


Figure 22: Initial and generated crack length vs wedge displacement curves for Mode#1 Small Scale Test

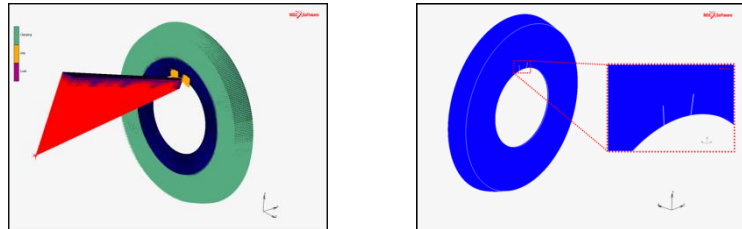


Figure 23: 3D FEM representative of Mode#3 Small Scale Test

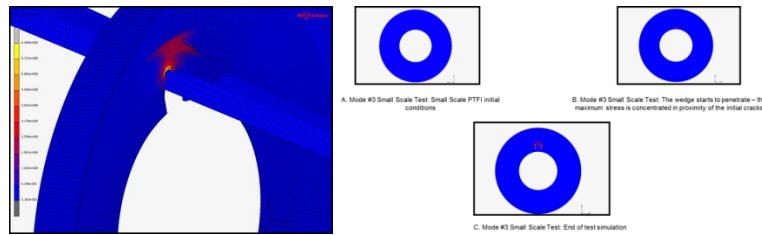


Figure 24: FEM results for Mode#3 Small Scale Test



Figure 25: Crack shape and final crack length for Mode#3 break: numerical vs experimental results

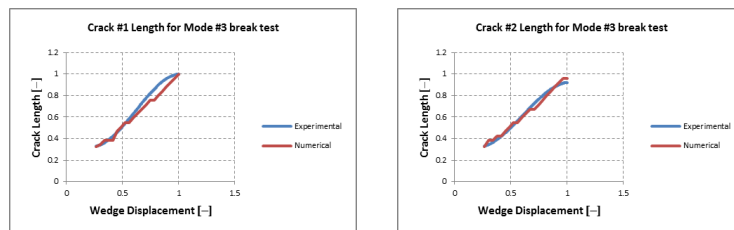


Figure 26: Crack#1 and Crack #2 length vs wedge displacement curves for Mode#3 Small Scale Test

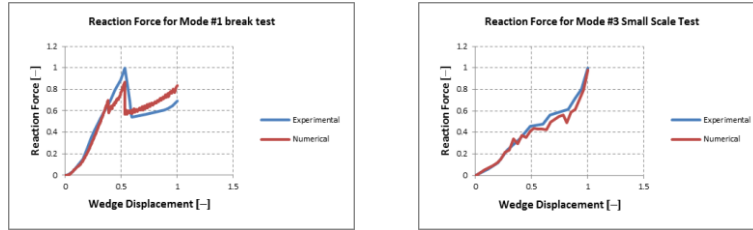


Figure 27: Reaction force vs wedge displacement curves for Mode#1 (on the left) and #3 (on the right) Small Scale Tests

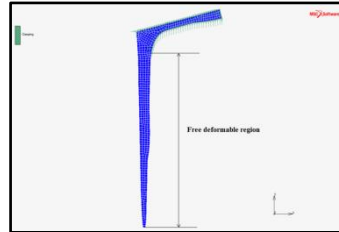


Figure 28: PTFI clamping conditions for the dimensioning configuration with closed floater

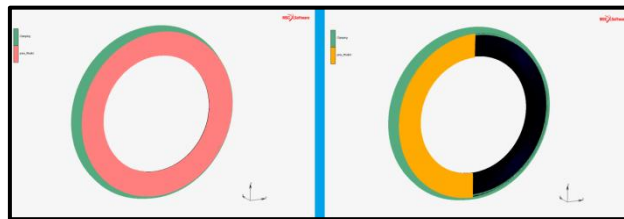


Figure 29: Loads applied on the Full Scale PTF numerical model

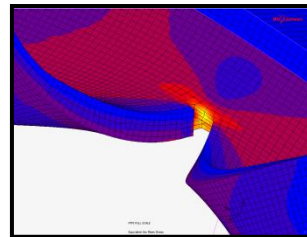


Figure 30: Stress distribution and crack propagation on PTF 3D FEM References

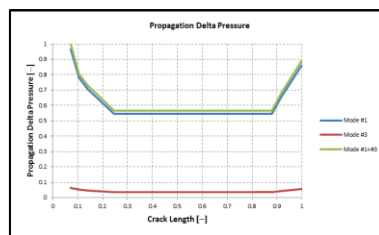


Figure 31: Propagation Delta Pressure vs Crack Length for ARTA05 PTF in configuration with closed floater

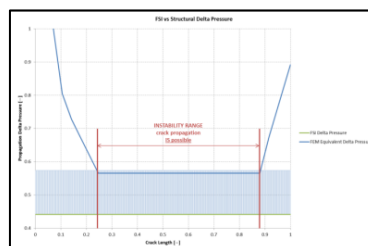


Figure 32: FSI and Structural Delta Pressure cross-check

Table 1: Test matrix for rubber Tensile

Test Type	Mode	Nominal Thickness [mm]	Specimens	T [°C]	v <sub>m</sub> [mm/min]	Output
Tensile	none	2	5	23 ± 2	500	σ (MPa) vs ε Curve
		4	5	23 ± 2	500	σ (MPa) vs ε Curve
		5	5	23 ± 2	500	σ (MPa) vs ε Curve

Table 2: Test matrix for rubber Tearing Mode #1 &amp; #3

Test Type	Mode	Nominal Thickness [mm]	Specimens	T [°C]	v <sub>m</sub> [mm/min]	Output
Tearing	#1	2	5	23 ± 2	500	F(N) vs s(mm) Curve
		4	5	23 ± 2	500	F(N) vs s(mm) Curve
		5	5	23 ± 2	500	F(N) vs s(mm) Curve
Tearing	#3	2	5	23 ± 2	50	F(N) vs s(mm) Curve
		4	5	23 ± 2	50	F(N) vs s(mm) Curve
		5	5	23 ± 2	50	F(N) vs s(mm) Curve

Table 3: Maximum differences between numerical and experimental data for both Mode #1 and #3 Tearing Tests

Mode of break	Thickness [mm]	Maximum Difference Δ [%]
#1	2	5
	4	3
	5	9
#3	2	10
	4	8
	5	6

Table 4: Maximum differences between numerical and experimental results for Mode #1 and #3 Small Scale Tests

	Mode #1 Maximum Δ [%]	Mode #3 Maximum Δ [%]
Final Cracks Length	14.06	4.83
Crack Length vs Wedge Displacement curves	25	11.91
Reaction Force vs Wedge Displacement curves	23.91	20.27

## References

- [1] ASTM D412, Test Methods for Vulcanized Rubber and Thermoplastic Rubbers and Thermoplastic Elastomers – Tension. Magin, T., and G. Degrez. 2004. Transport algorithms for partially ionized and unmagnetized plasmas. *J. Comput. Phys.* 198:424–449.
- [2] ASTM D624-00, Standard Test Method for Tear Strength of Conventional Vulcanized Rubber and Thermoplastic Elastomers..
- [3] ASTM D3182, Practice for Rubber– Materials, Equipment, and Procedures for Mixing Standard Compounds and Preparing Standard Vulcanized Sheets.
- [4] MSC.Marc Volume A, Theory and User Information, Version 2012.